Two-photon ionization of lithium in the time-dependent Hartree-Fock approximation

M. S. Pindzola and T. W. Gorczyca
Department of Physics, Auburn University, Auburn, Alabama 36849

C. Bottcher
Physics Division, Oak Ridge National Laboratory, Oak Ridge, Tennessee 37830
(Received 11 January 1993)

The two-photon ionization rate for the lithium atom is calculated in the time-dependent Hartree-Fock approximation for a variety of intensities and photon frequencies. The time-dependent equation for the valence Hartree-Fock orbital is solved on a two-dimensional cylindrical-coordinate lattice using both fixed and variable grid spacings. The nonperturbative results are compared with previous perturbation-theory results at photon energies near the $2s \rightarrow 3p$ single-photon resonance.

PACS number(s): 32.80.Rm

I. INTRODUCTION

With the development of high-intensity lasers that can exert forces on electrons in atoms equal to those that bind the atom, new theoretical methods [1] have been developed that treat this essentially nonperturbative problem. A promising approach is the application of time-dependent Hartree-Fock (TDHF) theory on a space-time lattice. The direct solution of the TDHF equations has been used to study heavy-ion collisions in nuclear physics [2], as well as atomic photoabsorption [3], ion-atom collisions [4–6], and ion-metal scattering [7]. Application of the TDHF method to nuclear physics centers around numerical methods tailored to rapidly varying short-range potentials. Complicating the application of the TDHF method to atomic physics has been the long-range nature of the electromagnetic interaction, and the consequent need to consider a very large spatial lattice.

In this paper we examine the direct solution of the TDHF equations for the two-photon ionization of lithium. For the case of lithium, which has one electron outside a closed shell, the TDHF equations may be solved in a frozen-core approximation, thus avoiding the need to solve a Poisson equation for the mean-field potential at each time step. To study two-photon ionization rates from the $2s$ subshell of lithium under linear polarized light, we employ a standard finite-difference solution on a two-dimensional (2D) lattice. To address the long-range Coulomb problem, we examine the extension of uniform grid methods to those employing variable mesh spacings. A key finding of this paper is that the implementation of a variable grid method is straightforward and leads to improved numerical accuracy. Following the development of the specific numerical method in Sec. II, we compare our 2D uniform and non-uniform mesh results with each other and with previous perturbation theory calculations in Sec. III. A brief summary is found in Sec. IV.

II. THEORY

For the single configuration $1s^2 2s$ of lithium, the time-dependent Hartree-Fock equation for the valence orbital is given by (atomic units are used)

$$\frac{i\partial\Psi_{2s}(\mathbf{r},t)}{\partial t} = \left[-\frac{1}{2}\nabla^2 - \frac{3}{r} + V(r) + E(t)z\sin\omega t\right]\Psi_{2s}(\mathbf{r},t) , \quad (1)$$

where $V(r)$ includes the electrostatic interaction with a frozen core $1s^2$ shell, $E(t)$ is the amplitude, and ω is the frequency of the electromagnetic field. If one sets the wave function $\Psi(\mathbf{r},t)=\Psi(\rho,z,t)e^{im\phi}/\sqrt{\rho}$, the TDHF equation may be solved in cylindrical coordinates (ρ,z,ϕ), where ϕ is ignored. Discretizing space and application of the variational principle to the energy functional yields the finite-difference equations [8],

$$\frac{i\partial\psi_{ij}(t)}{\partial t} = (H_\rho + H_z)\psi_{ij}(t) , \quad (2)$$

where for a uniform mesh

$$H_\rho\psi_{ij}(t) = -\frac{1}{2}\left\{\frac{(\rho_i+\Delta\rho/2)}{\sqrt{\rho_i\rho_{i+1}}}\frac{\psi_{i+1,j}(t)}{(\Delta\rho)^2} + \frac{(\rho_i-\Delta\rho/2)}{\sqrt{\rho_i\rho_{i-1}}}\frac{\psi_{i-1,j}(t)}{(\Delta\rho)^2} - \frac{2\psi_{ij}(t)}{(\Delta\rho)^2}\right\} + \frac{1}{2}\left[U_{ij}(t) + \frac{m^2}{2\rho_i^2}\right]\psi_{ij}(t) , \quad (3)$$

$$H_z\psi_{ij}(t) = -\frac{1}{2}\left\{\frac{\psi_{i,j+1}(t)}{(\Delta z)^2} + \frac{\psi_{i,j-1}(t)}{(\Delta z)^2} - \frac{2\psi_{ij}(t)}{(\Delta z)^2}\right\} + \frac{1}{2}\left[U_{ij}(t) + \frac{m^2}{2\rho_i^2}\right]\psi_{ij}(t) . \quad (4)$$

In Eqs. (2)–(4), $\psi_{ij}=\psi(\rho_i,z_j)$ and $U_{ij}(t)$ is the combined atom and field potential. The quantities $\Delta\rho$ and Δz are the lattice distances between successive points in ρ and z.

On the other hand, for a nonuniform mesh,

$$H_\rho\psi_{ij}(t)=-\frac{1}{2}\left\{\frac{(\rho_i+\Delta\rho_{i+1}/2)}{\sqrt{\rho_i\rho_{i+1}}}\frac{(\Delta\rho_{i+2}+\Delta\rho_{i+1})}{(\Delta\rho_{i+1}+\Delta\rho_i)}\frac{\psi_{i+1,j}(t)}{(\Delta\rho_{i+1})^2}+\frac{(\rho_i-\Delta\rho_i/2)}{\sqrt{\rho_i\rho_{i-1}}}\frac{\psi_{i-1,j}(t)}{(\Delta\rho_i)^2}\right.$$
$$\left.-\left[\frac{(\rho_i+\Delta\rho_{i+1}/2)}{\rho_i}\frac{(\Delta\rho_{i+2}+\Delta\rho_{i+1})}{(\Delta\rho_{i+1}+\Delta\rho_i)(\Delta\rho_{i+1})^2}+\frac{(\rho_i-\Delta\rho_i/2)}{\rho_i(\Delta\rho_i)^2}\right]\psi_{ij}(t)\right\}+\frac{1}{2}\left[U_{ij}(t)+\frac{m^2}{2\rho_i^2}\right]U_{ij}(t)\ , \tag{5}$$

$$H_z\psi_{ij}(t)=-\frac{1}{2}\left\{\frac{(\Delta z_{j+2}+\Delta z_{j+1})}{(\Delta z_{j+1}+\Delta z_j)}\frac{\psi_{i,j+1}(t)}{(\Delta z_{j+1})^2}+\frac{\psi_{i,j-1}(t)}{(\Delta z_j)^2}-\left[\frac{(\Delta z_{j+2}+\Delta z_{j+1})}{(\Delta z_{j+1}+\Delta z_j)(\Delta z_{j+1})^2}+\frac{1}{(\Delta z_j)^2}\right]\psi_{ij}(t)\right\} \tag{6}$$
$$+\frac{1}{2}\left[U_{ij}(t)+\frac{m^2}{2\rho_i^2}\right]\psi_{ij}(t)\ .$$

The quantities $\Delta\rho_i$ and Δz_j are the lattice distances between the points (ρ_i,z_j) and the points (ρ_{i-1},z_j) and (ρ_i,z_{j-1}), respectively. For a uniform mesh the matrices H_ρ and H_z are symmetric, but for a nonuniform mesh the matrices are nonsymmetric. The latter causes no difficulties since the numerical quadrature used for the energy functional and all other observables is well-defined for a nonuniform mesh. Stated another way, the nonsymmetric matrices on a nonuniform mesh may be transformed by the matrices

$$S_{ij}=\left[\frac{2}{\Delta\rho_i+\Delta\rho_{i+1}}\right]^{1/2}\delta_{ij}\ , \tag{7}$$

and

$$T_{ij}=\left[\frac{2}{\Delta z_i+\Delta z_{i+1}}\right]^{1/2}\delta_{ij}\ , \tag{8}$$

to obtain the symmetric matrices $S^{-1}H_\rho S$ and $T^{-1}H_zT$. Observables calculated with the time-dependent solutions of $S^{-1}H_\rho S$ and $T^{-1}H_zT$ would then have numerical quadrature weights of unity, and would equal those directly obtained from H_ρ and H_z.

The time evolution of the wave function in Eq. (1) may be approximated by the implicit expression [8]

$$\psi_{ij}(t)=\left[1+\frac{i\Delta t}{2}H_\rho\right]^{-1}\left[1+\frac{i\Delta t}{2}H_z\right]^{-1}\left[1-\frac{i\Delta t}{2}H_z\right]$$
$$\times\left[1-\frac{i\Delta t}{2}H_\rho\right]\psi_{ij}(t_0)\ , \tag{9}$$

where the time step $\Delta t=t-t_0$ is much less than ω^{-1}. Explicit expressions based on the Taylor expansion of the time evolution operator, $\exp(-i\Delta tH)$, may be used, but only with time steps a factor of 5 or more smaller than those used in Eq. (9).

After calculating bound-state orbitals in the Hartree-Fock approximation [9], the atomic potential for Eq. (1) may be constructed as a sum of the Hartree potential and a local exchange potential, $V_x(r)$, given by [10]

$$V_x(r)=-\frac{1}{2}\left[\frac{24}{\pi}\right]^{1/3}\{[\sigma(r)+\sigma_{2s}(r)]^{1/3}-[2\sigma_{2s}(r)]^{1/3}\}\ , \tag{10}$$

when $\sigma(r)$ is the total probability density for the atom and $\sigma_{2s}(r)$ is the probability density of the $2s$ electron. The initial wave function, $\Psi_{2s}(\mathbf{r},0)$, on the lattice is obtained by solving Eq. (1) in imaginary time, making sure the wave function remains orthogonal to all the same symmetry orbitals. Starting from the Hartree-Fock $2s$ orbital [9], convergence to the lattice function is usually achieved in 10–20 time steps. For propagation in real time, an imaginary absorbing potential is added to $V(r)$ of Eq. (1) to remove flux at the boundary of the lattice. Typically, $\Psi_{2s}(\mathbf{r},t)$ is propagated for 6000 time steps representing 30 optical cycles. The radiation field is turned on slowly by setting $E(t)=E_0t/t_{\max}$ with $t_{\max}=10$ optical cycles. An ionization rate is calculated from the decay of the norm of the wave function once the full intensity is reached.

III. RESULTS

Two-photon ionization rates for Lithium are obtained by solving Eq. (1) on both a uniform and nonuniform mesh. The 2D uniform spatial grid is 20.0×25.0 and contains 1.0×10^5 grid points with grid spacing $\Delta\rho=\Delta z=0.1$. The 2D nonuniform spatial grid is 19.5×24.5 and contains 1.4×10^5 grid points with grid spacing doubling five times from $\Delta\rho=\Delta z=0.0125$ to $\Delta\rho=\Delta z=0.2$. The ionization energy of the $2s$ wave function is given in Table I for both lattices. The use of a nonuniform mesh has substantially improved the agreement between the lattice ionization energy and that of the Hartree-Fock energy and experiment [11]. By halving the grid spacing of the 2D uniform mesh a more accurate ionization energy could be obtained, but only at the computational cost of a factor-of-4 increase in the number of grid points.

The application of standard perturbation theory results in a two-photon ionization rate $R_\alpha^{(2)}$, given by [12]

TABLE I. Ionization energies for lithium.

Method	Ionization energy (eV)
Hartree-Fock	5.34
TDHF (uniform)	5.57
TDHF (nonuniform)	5.33
Experiment (Ref. [11])	5.39

$$R_{\alpha}^{(2)}=\frac{16\pi^2 I^2}{c^2 k}\left|\sum_n \frac{\langle\psi_k|\hat{D}|\psi_n\rangle\langle\psi_n|\hat{D}|\psi_\alpha\rangle}{\varepsilon_\alpha-\varepsilon_n+\omega}\right|^2 , \quad (11)$$

where I is the intensity, c is the speed of light, k is the wave number of the photoelectron, and $\hat{D}$ is the length form of the dipole operator. The continuum normalization is one times a sine function. The perturbation-theory results of Mizuno [13], McGuire [14], and Edwards [15] for lithium, based on Eq. (11), are in good agreement and are presented in Fig. 1 for frequencies in the vicinity of the $2s\rightarrow 3p$ one-photon resonance and for an intensity of 10^{13} W/cm^2. The energies in the denominator of Eq. (11) have been adjusted [13–15] to the experimental resonance value of 3.83 eV [11].

The lowest-order perturbation-theory calculations are not applicable at very high intensities or on resonance. The $3p$ resonance in Li is broadened by single-photon Rabi cycling to the $2s$ ground state,

$$\Omega_{\alpha\beta}=\left[\frac{8\pi I}{c}\right]^{1/2}\langle\psi_\beta|\hat{D}|\psi_\alpha\rangle , \quad (12)$$

and single-photon ionization to the continuum,

$$\Gamma_{\alpha k}=\frac{8\pi I}{ck}|\langle\psi_k|\hat{D}|\psi_\alpha\rangle|^2 . \quad (13)$$

The energy positions of the ground and excited states may also be affected by ac Stark shifts,

$$\Delta_\alpha=\frac{2\pi I}{\omega c}\sum_{m=\pm 1}\sum_n \frac{|\langle\psi_n|\hat{D}|\psi_\alpha\rangle|^2}{\varepsilon_\alpha-\varepsilon_n+m\omega} . \quad (14)$$

For lithium at the $2s\rightarrow 3p$ resonance energy, and for an intensity of 10^{13} W/cm^2, we find that the Rabi cycling rate $\Omega_{2s\rightarrow 3p}=0.05$ eV, and the photoionization rate $\Gamma_{3p\rightarrow kl}=0.05$ eV. Using the Dalgarno-Lewis method to sum over intermediate states, we also calculate that $\Delta_{2s}=0.05$ eV and $\Delta_{3p}=0.12$ eV. We thus expect that nonperturbative TDHF calculations for the two-photon ionization of lithium, also at an intensity of 10^{13} W/cm^2, should yield a resonance width of around 0.1 eV and only a small change in the resonance peak position due to ac Stark shifts.

In Fig. 1 the TDHF ionization rates for lithium, at a fixed intensity of 1.0×10^{13} W/cm^2, are compared to second-order perturbation theory in the vicinity of the $2s\rightarrow 3p$ one-photon resonance. The differences between the TDHF resonance energies and experiment are comparable to the ionization energy differences reported in Table I. The nonuniform mesh results are again found to be superior. The line-shape width of the TDHF results (note the log scale for the ionization rate) is in reasonable

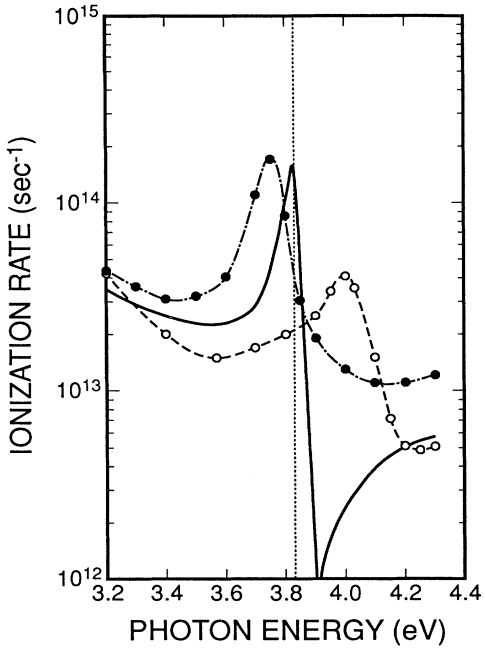

FIG. 1. Two-photon ionization of lithium near the $2s\rightarrow 3p$ one-photon resonance at an intensity of 10^{13} W/cm^2. Solid curve, second-order perturbation theory; dashed curve, TDHF theory with uniform mesh; chain-dashed curve, TDHF theory with nonuniform mesh. The $2s\rightarrow 3p$ excitation energy is indicated by the dotted line (Ref. 11).

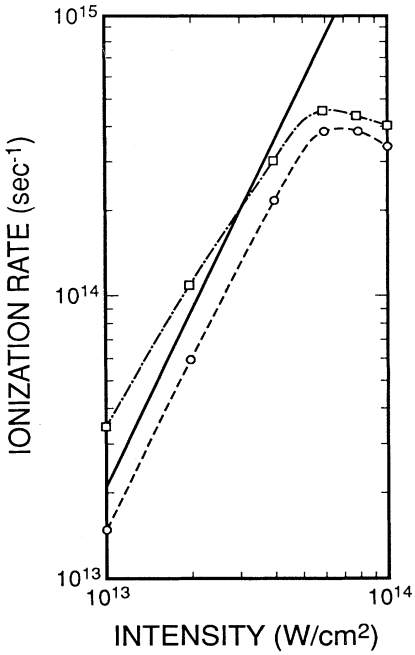

FIG. 2. Ionization of lithium at a photon frequency of 3.57 eV (ruby laser second harmonic). Solid curve, second-order perturbation theory; dashed curve, TDHF theory with uniform mesh; chain-dashed curve, TDHF theory with nonuniform mesh.

agreement with that due to Rabi cycling and excited-state photoionization. The antiresonance feature at 3.9 eV in the perturbation-theory results has also been quenched in the TDHF calculations, a characteristic of nonperturbative methods [16].

The TDHF line-shape curves at higher intensities will further broaden and will also show a shift in the resonance peak position due to stronger ac Stark shifts; the perturbation-theory expression of Eq. (14) yields $\Delta_{3p}=1.24$ eV at 1.0×10^{14} W/cm^2. Pronounced asymmetries in the line shape should also develop, in analogy with those found for hydrogen [17] and helium [18]. In Fig. 2 the TDHF ionization rates for lithium, at a fixed photon energy of 3.57 eV (ruby laser second harmonic), are compared to second-order perturbation theory. The TDHF curves of Fig. 2 track the I^2 dependence of the perturbation-theory results until about 6.0×10^{13} W/cm^2, where there follows a sharp departure for higher intensities. Plateau features in the rate versus intensity curve for hydrogen [17,19] were attributed to the appearance of a complicated spectrum of ac Stark shifted excited states, undoubtedly the case found here for lithium.

IV. SUMMARY

The accuracy of atomic photoabsorption calculations employing 2D TDHF methods has been shown to be significantly enhanced by the use of nonuniform grids. A path now lies open for the calculation of atomic collision dynamics in which one begins with an atomic structure containing all the core orbitals, represented by a grid adjusted to their widely different spatial extents. The standard technology of polarization potentials and spin-orbit interactions may then be invoked directly to obtain accurate energies and ionization rates. The great strength of the TDHF space-time lattice method remains its potential application to a wide variety of phenomena in atomic, nuclear, and particle physics.

ACKNOWLEDGMENTS

This research was supported by the National Science Foundation under Grant No. PHY-9122199 with Auburn University and by the U. S. Department of Energy under Contract No. DE-AC05-84OR21400 with Martin Marietta Energy Systems, Inc.

[1] J. Opt. Soc. Am. B **7**, 403 (1990), special issue on the theory of high-order processes in atoms in intense laser fields.
[2] K. T. R. Davies, K. R. S. Devi, S. E. Koonin, and M. R. Strayer, in *Treatise on Heavy Ion Science,* edited by D. A. Bromley (Plenum, New York, 1985), Vol. 3, p. 3.
[3] K. C. Kulander, K. J. Schafer, and J. L. Krause, in *Atoms in Intense Laser Fields,* edited by M. Gavrila (Academic, New York, 1992), p. 247.
[4] V. Maruhn-Rezwani, N. Grün, and W. Scheid, Phys. Rev. Lett. **43**, 512 (1979).
[5] C. Bottcher, Phys. Rev. Lett. **48**, 85 (1982).
[6] J. D. Garcia, Nucl. Instrum. Methods Phys. Res. A **240**, 552 (1985).
[7] K. J. Schafer, N. H. Kwong, and J. D. Garcia, Comput. Phys. Commun. **63**, 306 (1991).
[8] S. E. Koonin, K. T. R. Davies, V. Maruhn-Rezwani, H. Feldmeier, S. J. Krieger, and J. W. Negele, Phys. Rev. C **15**, 1359 (1977).
[9] C. F. Fischer, Comput. Phys. Commun. **14**, 145 (1978).
[10] I. Lindgren, Int. J. Quantum Chem. Symp. **5**, 411 (1971); A. Rósen and I. Lindgren, Phys. Scr. **6**, 109 (1972).
[11] C. E. Moore, *Atomic Energy Levels,* Natl. Bur. Stand. (U.S.) Circ. No. 35 (U.S. GPO, Washington, DC, 1971), Vol. I.
[12] F. H. M. Faisal, *Theory of Multiphoton Processes* (Plenum, New York, 1987).
[13] J. Mizuno, J. Phys. B **6**, 314 (1973).
[14] E. J. McGuire, Phys. Rev. A **23**, 186 (1981).
[15] M. Edwards, Phys. Rev. A **46**, 7228 (1992).
[16] S. I. Chu and W. P. Reinhardt, Phys. Rev. Lett. **39**, 1195 (1977).
[17] M. S. Pindzola and M. Dörr, Phys. Rev. A **43**, 439 (1991).
[18] M. D. Perry, A. Szoke, and K. C. Kulander, Phys. Rev. Lett. **63**, 1058 (1989).
[19] M. Dörr, R. M. Potvliege, and R. Shakeshaft, Phys. Rev. A **41**, 558 (1990).